Computational fluid dynamics simulations guided by Fourier velocity encoded MRI

Vinicius de Carvalho Rispoli* (vrispoli@pgea.unb.br)
Jon-Fredrik Nielsen† (jfnielse@umich.edu)
Krishna Nayak‡ (knayak@usc.edu)
Joao Luiz Azevedo de Carvalho* (joaoluiz@pgea.unb.br)

*Electrical Engineering, University of Brasilia, Brazil – †Biomedical Engineering, University of Michigan, USA
‡Electrical Engineering, University of Southern California, USA

PGEA — PÓS-GRADUAÇÃO EM ENGENHARIA DE SISTEMAS ELETRÔNICOS E DE AUTOMAÇÃO

GPSIM — Grupo de Processamento de Sinais e Imagens Médicas

Introduction

- Fourier velocity encoding (FVE) [1] provides considerably higher SNR than phase contrast (PC), and is robust to partial-volume effects [2].
- FVE data can be rapidly acquired, and low spatial resolution is tolerated [3,4].
- FVE provides the velocity distribution associated with a large voxel, but does not directly provides a velocity map.
- CFD can be an alternative to (or combined with) MR flow quantification [5]
- CFD has arbitrary SNR and spatio-temporal resolution
- **Goal**: derive high-resolution velocity maps from simulated low-resolution FVE data [6] and use it to perform guided CFD simulations [5].

Estimating the velocity map

- FVE spatial-velocity distribution, $s(x,y,w)$, model is:

$$s(x,y,w) = \left[m(x,y) \times \operatorname{sinc}\left(\frac{w - w_{\mathrm{pc}}(x,y)}{\delta w}\right)\right] * \mathrm{psf}\left(\frac{r}{\delta r}\right) \quad (1)$$

- Spatial blurring effects in FVE data are reduced, using the deconvolution algorithm proposed in ref. [7]:

$$\tilde{s}(x,y,w) \approx m(x,y) \times \operatorname{sinc}\left(\frac{w - w_{\mathrm{pc}}(x,y)}{\delta w}\right). \quad (2)$$

- Given a high-resolution spin-density map, $\tilde{m}(x,y)$, velocity $\hat{w}_{\mathrm{fve}}$ at (x_o, y_o) is estimated from $\tilde{s}(x,y,w)$ as:

$$\hat{w}_{\mathrm{fve}}(x_o,y_o) = \arg\min_{\omega} \left\| \frac{\tilde{s}(x_o,y_o,w)}{\tilde{m}(x_o,y_o)} - \operatorname{sinc}\left(\frac{w-\omega}{\delta w}\right)\right\|_2 \quad (3)$$

Numerical Procedure

- Navier–Stokes equation,

$$\rho\left(\frac{\partial \boldsymbol{\nu}}{\partial t} + \boldsymbol{\nu}\cdot\nabla\boldsymbol{\nu}\right) = -\nabla p + \mu\Delta\boldsymbol{\nu}, \quad (4)$$

  is numerically solved with a modified SIMPLER algorithm [5].
- Discretization of the Navier-Stokes equation yelds three linear systems:

$$\mathbf{S}_{\nu,i}\boldsymbol{\nu}_{i+1} = \mathbf{f}_{\nu,i}, \quad (5)$$

  for each velocity component $\boldsymbol{\nu} = \mathbf{u}$, $\mathbf{v}$ or $\mathbf{w}$.
- Approach [5]: solve the modified linear systems

$$\boldsymbol{\nu}_{i+1} = (\mathbf{S}_{\nu,i}^T\mathbf{S}_{\nu,i} + \lambda_\nu \boldsymbol{\Gamma}_\nu^T\boldsymbol{\Gamma}_\nu)(\mathbf{S}_{\nu,i}^T\mathbf{f}_{\nu,i} + \lambda_\nu\boldsymbol{\Gamma}_\nu^T\boldsymbol{\nu}_{\mathrm{mri}}), \quad (6)$$

  which corresponds to the optimal solution of the following regularization

$$J(\boldsymbol{\nu}_{i+1}) = \frac{1}{2}||\mathbf{S}_{\nu,i}\boldsymbol{\nu}_{i+1} - \mathbf{f}_{\nu,i}||^2 + \frac{\lambda_\nu}{2}||\boldsymbol{\Gamma}_\nu\boldsymbol{\nu}_{i+1} - \boldsymbol{\nu}_{\mathrm{mri}}||^2. \quad (7)$$

- $\boldsymbol{\Gamma}_\nu$ adjusts the size of vector $\boldsymbol{\nu}_{i+1}$ to that of $\boldsymbol{\nu}_{\mathrm{mri}}$, and λ_ν controls the weight of the regularization.
- Obtained solution is the best one that fits both Navier–Stokes and the MRI data.

Experiments

- 3D PC-MRI data were acquired for a carotid flow phantom (Fig.1).
  - Voxel: $0.5 \times 0.5 \times 1.0$ mm^3; FOV: $4.0 \times 3.5 \times 5.0$ cm^3; NEX: 9; Venc: 50 cm/s.
- Spiral FVE data were simulated from PC-MRI, using $\delta r = 1$mm and $\delta r = 2$mm ($\mathrm{SNR}_{\mathrm{fve}} > \mathrm{SNR}_{\mathrm{pc}}$)
- $\hat{w}_{\mathrm{fve}}$ maps were reconstructed from simulated FVE
- FVE-guided CFD velocity fields were compared with:
  - Pure CFD solution;
  - PC-guided CFD velocity field obtained using a single NEX of the PC scan (same scan time as FVE scan with $\delta r = 1$mm)
  - PC-guided CFD velocity field obtained using all 9-NEX of the PC scan

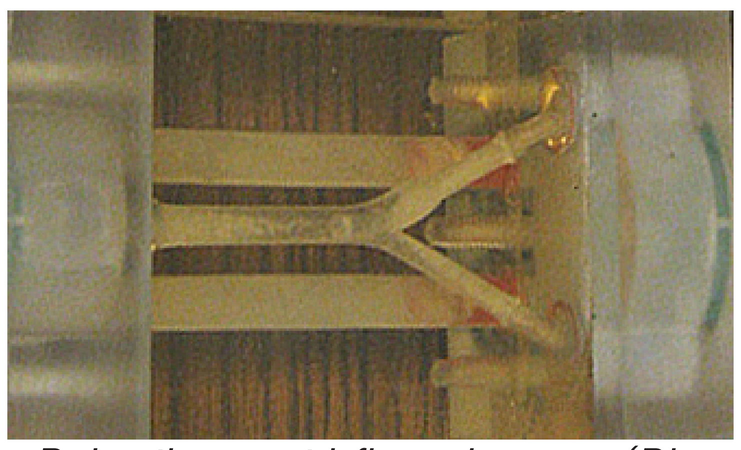

Figure 1: *Pulsatile carotid flow phantom (Phantoms by Design, Inc., Bothell, WA).*

Results and Conclusion

- Figure 2 presents the FVE-estimated velocity maps, $\hat{w}_{\mathrm{fve}}$. Abs. error was greater than 5 cm/s for:
  - 9% of the voxels for $\delta r = 1$ mm
  - 26.5% of the voxels for $\delta r = 2$ mm
- Figure 3 shows the PC-measured velocity field; and all CFD-simulated velocity fields: pure CFD, PC-driven CFD (1 and 9 NEX), and FVE-driven CFD ($\delta r = 1$ and 2 mm).
  - Considerable qualitative improvement for FVE-driven results, when compared with the pure CFD result and with PC-driven CFD with similar scan time (1 NEX).
- **Result 3**: Table 1 presents signal–to–error ratio (SER), relative to PC reference, for CFD results
  - Both FVE-driven solutions had higher SER than pure CFD and single-NEX PC-driven CFD
  - When evaluating 3D velocity vector $\vec{\nu}$, the SER gain for $\delta r = 1$ mm (similar scan time): was 1.49 dB relative to pure CFD; and 3.65 dB relative to single-NEX PC-driven CFD.
- **Conclusion**: Results show that FVE-guided CFD has better agreement with PC-measured velocity field than pure CFD.
  - 1 mm resolution spiral FVE dataset has same scan time as 1 NEX of a 0.5 mm resolution 3DFT PC dataset with same parameters
  - FVE dataset would have SNR 23 dB higher than that of PC

	pure CFD	CFD + 1D PC 1 NEX	CFD + sFVE $\delta r = 1.0$ mm
SER_u	2.97 dB	2.72 dB (↓)	3.93 dB (↑)
SER_v	−0.25 dB	−0.88 dB (↓)	−0.36 dB (↓)
SER_w	5.44 dB	6.21 dB (↑)	10.97 dB (↑↑)
$\mathrm{SER}_{\vec{\nu}}$	6.57 dB	4.41 dB (↓)	8.06 dB (↑)

Table 1: *Signal-to-error ratio between each of the CFD approaches and the PC reference.*

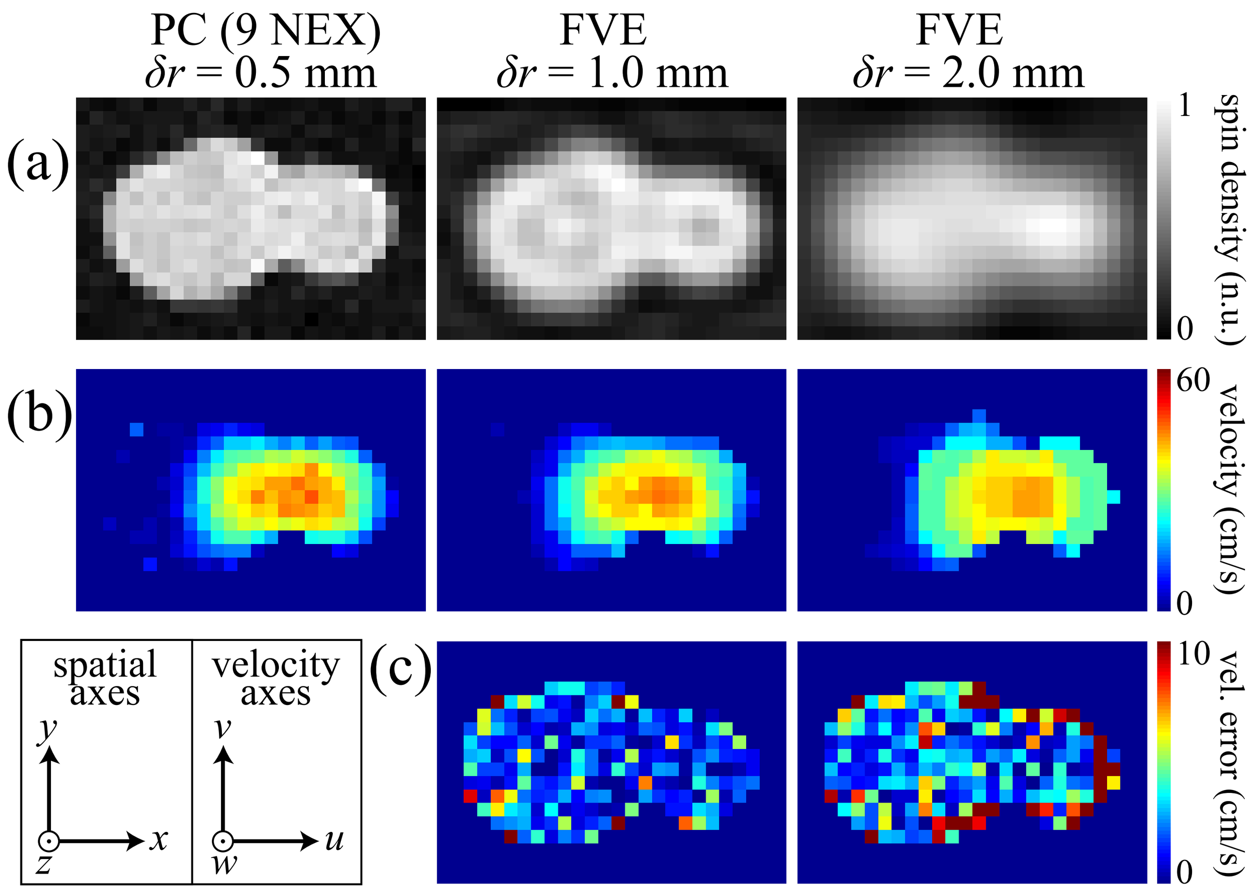

Figure 2: *(a) Spin-density maps for PC (0.5 mm spatial resolution, 9 NEX), FVE with 1 mm spatial resolution, and FVE with 2 mm spatial resolution, for a slice perpendicular to a carotid phantom's bifurcation; (b) corresponding velocity maps; and (c) absolute error for the FVE-estimated velocity maps, relative to the PC reference.*

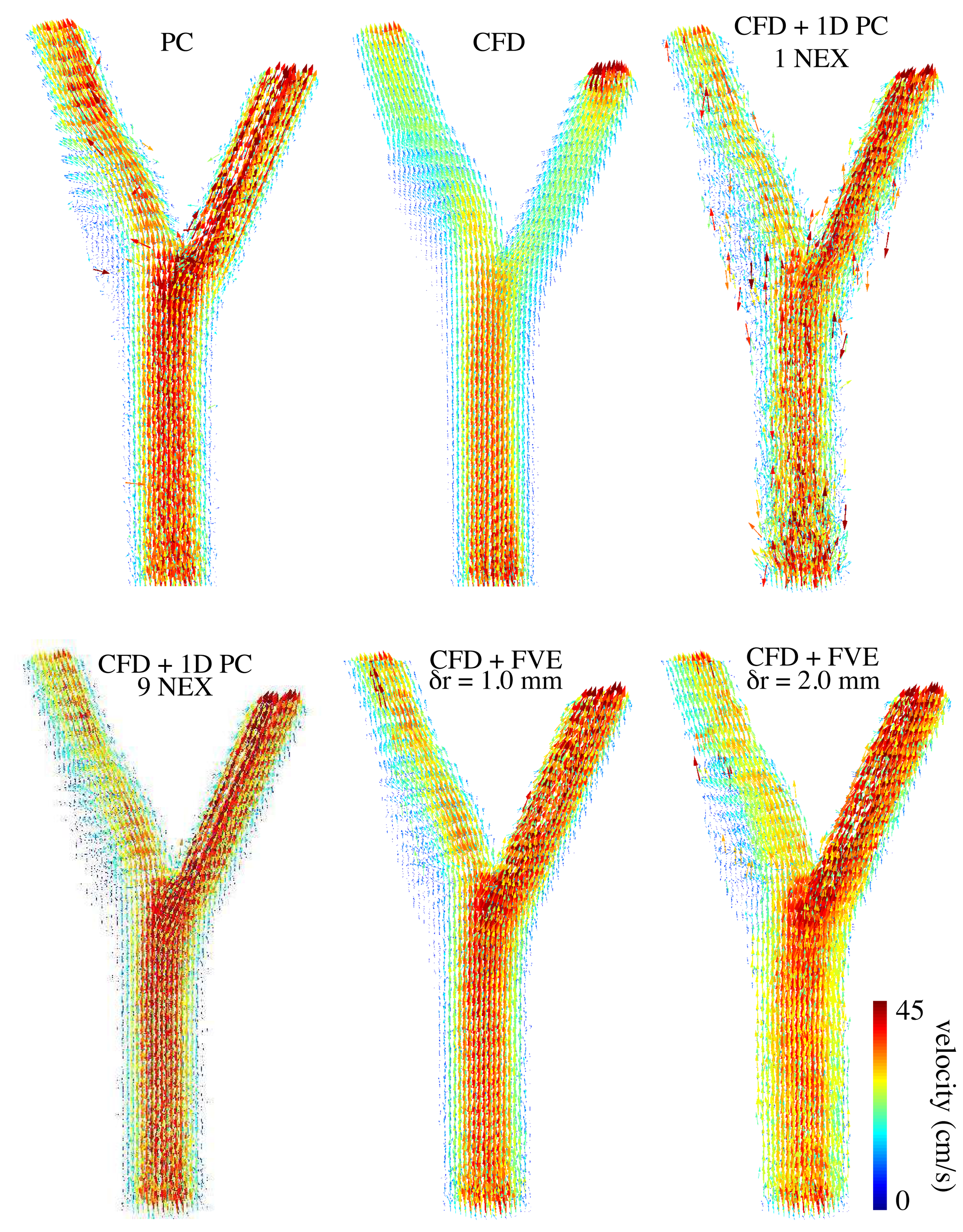

Figure 3: *Vector field visualization of the velocity field ($\vec{\nu}$) over the entire tridimensional volume of the carotid bifurcation of the phantom: PC; pure CFD; CFD guided by w_{pc}, reconstructed from 1 NEX and 9 NEX; CFD guided by $\hat{w}_{\mathrm{fve}}$, recovered from simulated FVE data with δr = 1.0 mm and 2.0 mm.*

References

[1] Moran PR. MRI 1:197, 1982.
[2] Tang C, et al. JMRI 3:377, 1993.
[3] Carvalho JLA and Nayak KS. MRM 57:639, 2007.
[4] Carvalho JLA, et al. MRM 63:1537, 2010.
[5] Rispoli VC, et al. Proc ISMRM 22: 2490, 20014.
[6] Rispoli VC and Carvalho JLA. ISBI 10: 334, 2013.
[7] Krishnan D and Fergus R. Proc 24th NIPS, 2009.